Published in final edited form as:
Neuroscience. 2013 March 1; 0: 226–238. doi:10.1016/j.neuroscience.2012.11.015.

$P2X_3$ and TRPV1 functionally interact and mediate sensitization of trigeminal sensory neurons

Jami L. Saloman, **Man-Kyo Chung**, and **Jin Y. Ro**[+]
University of Maryland Baltimore School of Dentistry, Department of Neural and Pain Sciences, Program in Neuroscience, 650 W. Baltimore Street, Baltimore, Maryland 21201, USA

Abstract

Musculoskeletal pain conditions, particularly those associated with temporomandibular joint and muscle disorders (TMD) affect a large percentage of the population. Identifying mechanisms underlying hyperalgesia could contribute to the development of new treatment strategies for the management of TMD and other muscle pain conditions. In this study, we provide evidence of functional interactions between two ligand-gated channels, $P2X_3$ and TRPV1, in trigeminal sensory neurons, and propose that the interactions serve as an underlying mechanism for the development of mechanical hyperalgesia. Mechanical sensitivity of the masseter muscle was assessed in lightly anesthetized rats via an electronic anesthesiometer (Ro et al., 2009). Direct intramuscular injection of a selective $P2X_3$ agonist, αβmeATP, induced a dose- and time-dependent hyperalgesia. Mechanical sensitivity in the contralateral muscle was unaffected suggesting local $P2X_3$ mediate the hyperalgesia. Anesthetizing the overlying skin had no effect on αβmeATP-induced hyperalgesia confirming the contribution of $P2X_3$ from muscle. Importantly, the αβmeATP-induced hyperalgesia was prevented by pretreatment of the muscle with a TRPV1 antagonist, AMG9810. $P2X_3$ was co-expressed with TRPV1 in masseter muscle afferents confirming the possibility for intracellular interactions. Additionally, in a subpopulation of $P2X_3$/TRPV1 positive neurons, capsaicin-induced Ca^{2+} transients were significantly amplified following $P2X_3$ activation. Finally, activation of $P2X_3$ induced phosphorylation of serine, but not threonine, residues in TRPV1 in trigeminal ganglia cultures. Significant phosphorylation was observed at 15 min, the time point at which behavioral hyperalgesia was prominent. Previously, activation of either $P2X_3$ or TRPV1 had been independently implicated in the development of mechanical hyperalgesia. Our data propose $P2X_3$ and TRPV1 interact in a facilitatory manner, which could contribute to the peripheral sensitization known to underlie masseter hyperalgesia.

Keywords

rat; trigeminal ganglia; masseter; mechanical hyperalgesia; αβmeATP

[+]**Send correspondence and proofs to:** Jin Y. Ro, Department of Neural and Pain Sci, Program in Neuroscience, University of Maryland Baltimore, School of Dentistry, 650 W. Baltimore St., Baltimore, Maryland 21201, USA, Phone: (410) 706-6027, Fax: (410) 706-4172, JRo@umaryland.edu.

1. Introduction

Patients with temporomandibular disorders (TMD) often suffer from mechanical hyperalgesia arising in masticatory muscles (Harness et al., 1990; Stohler, 1999). Transient Receptor Potential V1 (TRPV1) are increasingly recognized as important players underlying mechanical hyperalgesia (Pomonis et al., 2003; Walker et al., 2003; Honore et al., 2005; Fujii et al., 2008). Specifically in muscle, blocking TRPV1 attenuates mechanical hyperalgesia induced by eccentric muscle contraction (Fujii et al., 2008). Additionally, masseteric injection of the TRPV1 agonist capsaicin significantly lowers noxious mechanical thresholds in humans and rats (Arendt-Nielsen et al., 2008; Ro et al., 2009), which could result from sensitization of muscle nociceptors (Hoheisel et al., 2004).

TRPV1 function as signal integrators downstream of several pro-inflammatory G-protein coupled receptors (GPCRs) (Levine and Alessandri-Haber, 2007). In particular, TRPV1 functionally interact with the P2Y purinergic GPCRs. $P2Y_1$ potentiates TRPV1 in a PKC-dependent manner (Tominaga et al., 2001). $P2Y_2$ knockout (KO) mice exhibit deficits in capsaicin-induced Ca^{2+} transients and thermal hyperalgesia (Malin et al., 2008). Similarly, TRPV1 KO mice exhibit no ATP-induced thermal hyperalgesia. Selective activation of $P2Y_2$ potentiates capsaicin currents in dorsal root ganglia (DRG) neurons (Moriyama et al., 2003).

Recently, TRPV1 were also linked to the ionotropic purinergic receptor $P2X_3$ in DRG (Piper and Docherty, 2000; Stanchev et al., 2009). The channels co-immunoprecipitate when co-transfected in HEK293 cells (Stanchev et al., 2009). Alpha,beta-methyleneadenosine triphosphate (αβmeATP), a $P2X_3$ agonist used to simulate ATP release, restores the attenuation of TRPV1 expression in a PKC dependent manner in DRG following sympathectomy (Xu et al., 2010). These data suggest $P2X_3$ and TRPV1 interact at the cellular level.

$P2X_3$ have been implicated in craniofacial pain. Increased face wiping behavior following tooth movement was attenuated by the P2X antagonist TNP-ATP (Yang et al., 2009). Carrageenan or αβmeATP injections into the temporomandibular joint (TMJ) evoked nociceptive responses that were significantly blocked by co-injection with the P2X antagonist PPADS (Oliveira et al., 2005). In muscle, masseteric injection of αβmeATP dose-dependently reduced pressure pain threshold (Shinoda et al., 2008). Although the involvement of peripheral $P2X_3$ in craniofacial pain is evident the cellular mechanisms remain to be elucidated.

Recent studies in DRG have linked $P2X_3$ activation to Ca^{2+}-dependent kinases, which are known to sensitize TRPV1 (Bhave et al., 2003; Jung et al., 2004). Treatment of DRG cultures with ATP or αβmeATP resulted in translocation and increases in the phosphorylated form of CaMKII (Hasegawa et al., 2009). If $P2X_3$ are also co-expressed with TRPV1 in masseter afferents similar pathways could underlie $P2X_3$-induced hyperalgesia. Since a copious amount of ATP is released in the muscle during injury or inflammation (Reinohl et al., 2003; Hoheisel et al., 2004), we hypothesized that activation of

masseteric $P2X_3$ invokes signaling cascades that converge on TRPV1 producing mechanical hyperalgesia. We first reproduced and validated $P2X_3$-induced mechanical hyperaglesia in our orofacial muscle pain model. We then investigated whether (1) $P2X_3$-induced masseter mechanical hyperaglesia is TRPV1-dependent, (2) $P2X_3$ and TRPV1 co-express in masseter afferents, (3) $P2X_3$ activation enhances TRPV1 function in trigeminal ganglia (TG), and (4) $P2X_3$ activation leads to TRPV1 phosphorylation in TG.

2. Experimental Procedures

2.1 Animals

Male Sprague Dawley rats (100–150 and 300–350 gm; Harlan, Indianapolis) were used in the present study. A total of 153 rats were used to complete this study. All of the animals were housed in a temperature-controlled room under a 12:12 light-dark cycle with access to food and water ad libitum. All procedures were conducted in accordance with the NIH Guide for the Care and Use of Laboratory Animals (NIH Publications No. 80–23) and under a University of Maryland approved Institutional Animal Care and Use Committee protocol.

2.2 Behavioral Studies

Noxious chemical or mechanical stimulation of the masseter muscle evokes characteristic shaking of the ipsilateral hindpaw in lightly anesthetized rats (Ro et al., 2003; Han et al., 2008; Sanchez et al., 2010). We have previously described the use of this behavior for testing mechanical sensitivity of the masseter muscle in rats (Ro and Capra, 2006; Ro et al., 2007; Ro et al., 2009; Saloman et al., 2011). The lightly anesthetized model allows standardized delivery of drugs and repeated application of mechanical stimuli in deep craniofacial tissue such as the masseter or TMJ which is much more difficult in awake-behaving rats. Briefly, rats were initially anesthetized with an intraperitoneal (i.p.) injection of sodium pentobarbital (40 mg/kg). A level of ‘light’ anesthesia was determined by providing a noxious pinch to the tail or the hindpaw with a serrated forceps. Rats typically respond to the noxious pinch on the tail with an abdominal contraction and with a withdrawal reflex to the noxious pinch of a hindpaw about 15 min after the initial anesthesia. Once the animal reached this level a metal clip calibrated to produce 600 gm of force was applied 5 consecutive times, and experiments were continued only after the animals showed a reliable reflex response to every clip application. A tail vein was connected to an infusion pump (Harvard Apparatus, Pump11) for continuous infusion of pentobarbital. The rate of infusion was adjusted to maintain a relatively light level of anesthesia throughout the duration of the experiment (3 mg/hr).

The baseline mechanical threshold for evoking hindpaw responses was determined 15 min prior to drug injections using an electronic VF anesthesiometer (IITC Life Science, Inc, Woodland Hills, CA). A rigid tip (diameter 2 mm) attached to the VF meter was applied to the masseter muscle until the animals responded with hindpaw shaking. The animal’s head was rested flat against the surface of the table when pressing the anesthesiometer on the masseter in order to provide a stable set-up. The threshold was defined as the lowest force necessary to evoke the hindpaw response.

Changes in masseter sensitivity were then assessed at 15, 30, 45, 60 and 90 min following drug treatments. We calculated percent changes in VF thresholds following drug treatments with respect to the baseline threshold and plotted against time. In order to assess the overall magnitude of drug-induced changes in masseter sensitivity over time, the area under the curve (AUC) was calculated for the normalized data for each rat using the trapezoid rule. All animals were kept warm throughout the experiments with thermal blankets.

Data Analysis—For behavioral studies, the time-dependent mean percent changes in mechanical thresholds were normalized to the baseline threshold and analyzed with a two-way ANOVA with repeated measures. In addition, either the student t-test or one-way ANOVA was used to evaluate the overall magnitude of mechanical hyperalgesia assessed as AUC. All multiple group comparisons were followed by the appropriate post hoc test. The significance of these and all subsequent statistical analyses was set at $P < 0.05$.

2.3 Experimental and control groups for behavioral studies

To assess whether activation of $P2X_3$ induces mechanical hyperalgesia, the masseter muscle was treated with a specific $P2X_3$ agonist, αβmeATP, (250, 500, 750 μg/20 μl) or the vehicle. Doses were adapted from Shinoda et al. (2008). To confirm we are measuring the effect of $P2X_3$ activation on muscular sensitivity, a topical anesthetic (20% benzocaine) was applied to the skin overlying the muscle prior to injecting the masseter with 750 μg/20 μl αβmeATP. There is also a possibility that αβmeATP injected into the masseter can mediate its effects by activating centrally located $P2X_3$. In order to evaluate possible systemic effects, in a separate group of animals, the highest dose of αβmeATP (750 μg) was administered into the masseter contralateral to the muscle being tested for mechanical sensitivity. In order to confirm the specificity of αβmeATP effects, the masseter muscle was pretreated with a selective $P2X_3$ antagonist, A-317491. In this experiment A-317491 (7.5, 250 μg/10 μl) or the vehicle was injected 5 min prior to the αβmeATP (750 μg). Doses of A-317491 were adapted from Wu et al. (2004). In order to determine if TRPV1 are involved in $P2X_3$-mediated effects, animals were pretreated with a TRPV1 antagonist, AMG9810 (1, 10, 100 nmol/10 μl), or vehicle prior to αβmeATP (750 μg). In groups in which animals received multiple injections, the drugs were administered 5 min apart. The number of rats per group is indicated within the figures. In general, groups consisted of 6–8 rats, totaling 106 rats used in the behavioral studies. Further experiments examining the specificity of αβmeATP and AMG9810 were conducted using the Ca^{2+} Imaging technique and are described within the text.

2.4 Drug Preparation and Administration for Behavior Studies

αβmeATP (pH was adjusted to 7.0 using NaOH) and A-317491 (Sigma) were dissolved in PBS. AMG9810 (Tocris; Ellisville, MO, USA) was dissolved in 5% DMSO, 10% Tween-80, and 85% PBS (Ruparel et al., 2008). In order to make sure that the drugs and vehicles were administered in the same target region of the muscle the injection site was determined by palpating the masseter muscle between the zygomatic bone and the angle of the mandible. Injections were made with a 27-gauge needle. Upon contacting the mandible the needle was slowly withdrawn into the mid-region of the masseter and injections were made for 5–10 sec.

2.5 Labeling of Masseter Afferents and Immunohistochemistry

Initially, 4 rats were anesthetized with sodium pentobarbital (40 mg/kg, i.p.). Masseter muscles were exposed and 2% Fast Blue (FB; 10 μl) was injected bilaterally into multiple sites to retrogradely label muscle afferents. To avoid leakage the needle was left in place for 1–2 min before slow retraction. The injection site was then covered with petroleum jelly and sutured (4.0 silk). After 7 days, rats underwent transcardial perfusion with 4% paraformaldehyde in PBS (250 ml; pH 7.3). TG were extracted and post-fixed for 90 min, placed in 30% sucrose at 4°C overnight, and sectioned coronally at 12 μm. Alternate sections were collected and mounted on gelatin-coated slides. The sections were incubated overnight with primary antisera for TRPV1 (1:1000; Rabbit Cat# RA10110; Neuromics, Edina, MN) and $P2X_3$ (1:3000; Guinea pig Cat# AB5896; Millipore, Billerica, MA). For immunofluorescence, sections were incubated for 1 hr in Alexa 488 conjugated goat anti-rabbit antiserum (1:250; Invitrogen West Grove, PA) and Cy3 goat anti-guinea pig antiserum (1:250; Jackson ImmunoResearch, West Grove, PA) at room temperature. The primary antibodies for TRPV1 or $P2X_3$ were omitted from processing from select sections to control for non-specific staining. Trigeminal and facial motor nuclei were also evaluated as positive and negative controls for FB labeling, respectively.

The immunohistochemical data were analyzed using Image J (NIH) threshold analysis. Only the labeled neurons that showed a clear nucleus were included in the counting. The percentages of masseter afferents labeled with TRPV1 and/or $P2X_3$ were calculated and presented as mean ± standard error of the mean (SE). $P2X_3$/TRPV1/FB positive cells were also categorized according to size (small <400μm^2, medium 400–1000 μm^2, and large >1000 μm^2)(Chun et al., 2008).

The rabbit anti-TRPV1 corresponds to residues 4–21 of rat TRPV1 (RASLDSEESESPPQENSC). The specificity of the TRPV1 antibody has previously been established (Guo et al., 1999; Kim et al., 2008). Western blots and immunohistochemistry of DRG reveal staining colocalizes with a TRPV1 antibody targeting a different an entirely separate epitope (N-terminal) and preadsorption with peptide blocks the signal. Additionally, the antibody only detects signal in HEK293 cells transfected with TRPV1 as opposed to nontransfected cells. The guinea pig anti-$P2X_3$ (Lot# LV1518241) is a 15 amino acid peptide corresponding to amino acids 383–397 of the carboxy-terminus of rat $P2X_3$. The specificity of the $P2X_3$ antibody was previously confirmed in TG by preadsorption studies as well as omission of the antibody which abolished all specific staining (Guo et al., 1999; Kim et al., 2008). Antibodies against this epitope stain HEK293 cells transfected with $P2X_3$, but fail to stain untransfected cells (Vulchanova et al., 1997). The signal was abolished with peptide preadsorption.

2.6 Primary Culture of TG Neurons

Rat TG neurons were cultured as described previously (Lee et al., 2012; Wang et al., 2012) TG were extracted from 100–150 gm rats and minced in DMEM/F12 (Sigma) containing Horse Serum (HS) and penicillin/streptomycin/glutamine (PSG) on ice, incubated in media containing 1 mg/ml collagenase type XI (Sigma) for 30 min at 37°C with agitation. Following trituration, cells were incubated for 2 min in 0.05% Trypsin/0.1% EDTA at 37°C

with agitation. *For Ca^{2+} Imaging:* One rat (2 TG) was used for one culture and cells were separated via a Percoll gradient for 12 min at 900-g and plated on poly-L-ornithine and laminin-coated glass coverslips. The neurons were cultured in 2 ml DMEM (Gibco) containing HS and PSG at 37°C under 5% CO_2. 16–24 hrs later, cells were loaded with Fura2- acetoxymethyl ester (Fura2-AM) and pluronic acid (Anaspec Inc) for 40 min at 37°C. *For Immunoprecipitation:* TG from two rats were used for one culture and the cells were plated on laminin-coated 12-well plates. In this situation cultures were used for experimentation 48 hrs later. No growth factors or other additional supplements were included.

2.7 Ratiometric Ca^{2+} Imaging Study

Ratiometric Ca^{2+} imaging was performed as described previously (Lee et al., 2012; Wang et al., 2012). Primary TG cultures were loaded with 20 μl of 1 mM Fura2-AM and 2μl of 20% pluronic acid (Anaspec, Inc) for 40 min at 37°C in Calcium Imaging Buffer (CIB). CIB contained in mM: NaCl 130; KCl 3; $CaCl_2$ 2.5; $MgCl_2$ 0.6; 4-(2-hydroxyethyl)-1-piperazineethanesulfonic acid (HEPES) 10; Sucrose 10; $NaHCO_3$ 1.2 (pH 7.45, 320 mOsm adjusted with mannitol). Following a 15 min wash period for de-esterification, dual images (510 nm emission) were collected every 2 sec using NIS Elements (Nikon). The Fura response (FR) was defined as the ratio of background-subtracted emissions measured during excitation at 340 and 380 nm.

Drugs were diluted to final concentrations in CIB: αβmeATP (50 μM), capsaicin (10 nM, 1 μM), AMG9810 (1 μM), and A-317491 (500 nM, 1 μM, 3 μM). Stock solutions were generated as follows: αβmeATP and A-317491 10 mM in H_2O, capsaicin 10 mM in ethanol, and AMG9810 10 mM in DMSO.

Data Analysis—We calculated the changes in fura response (ΔFR, FR_{peak} minus $FR_{baseline}$) in every cell. Baseline was defined as the average of the five data points prior to a given stimulus application. A neuron was considered a responder if the Fura response to αβmeATP or capsaicin application was above threshold. Threshold was determined following a similar method reported in Chung et al., (2003). A histogram was generated from a population of neurons to a given stimulus protocol. The ΔFR greater than two standard deviations from the peak ΔFR of non-responding neurons was classified as responsive. The data were analyzed with two-way ANOVA with repeated measures, followed by Bonferroni's test. Non-parametric data were analyzed with a Kruskal-Wallis one-way ANOVA or Mann-Whitney test.

2.8 Immunoprecipitiation

Cultures were dissociated with Ripa lysis buffer (Cell Signaling; Danvers, Ma). Equal amounts of purified protein were incubated with 3 μl of TRPV1 antibody (Cat#PC420; Calbiochem; San Diego, CA) at 4°C overnight, and then the substrate/antibody complex was incubated with protein A/G Agarose beads (Santa Cruz Biotechnology; Santa Cruz, CA) for 2 hrs at 4°C. LDS sample buffer including SDS was added to elute proteins from the protein A/G beads. Samples were separated by 4–12% NuPage gel (Invitrogen; Carlsbad, CA) electrophoresis and subjected to immunoblotting. To assess the level of Ser and Thr

phosphorylation, membranes were treated with primary antibodies anti-phosphoserine 16B4 (1:1000; Santa Cruz) or anti-phosphothreonine 14B3 (1:1000; Chemicon) followed by the secondary antibody mouse IgG HRP (1:5000). Membranes were developed with Amersham ECL Plus reagents (GE HealthCare Life Science, Piscataway, NJ), then stripped and re-probed with anti-TRPV1 (1:1000; rabbit; Calbiochem) followed by rabbit-HRP (1:5000) to verify the amount of protein. The TRPV1 antibody was a purified rabbit polyclonal antibody directed against a synthetic peptide corresponding to amino acids 824–838 of rat TRPV1. The specificity of the anti-TRPV1 antibody has been tested previously in immunoprecipitation experiments as well as TRPV1 knockout tissue (Pabbidi et al., 2008).

Chemoluminscence was applied to visualize antigen-antibody complexes on blots that were exposed to X-ray film. Films were scanned and quantified using Image J Software (NIH). Phosphorylation signals were normalized to that of pan-TRPV1, which served as the control and confirmation of the TRPV1 band. The data was subjected to a one-way ANOVA. All multiple group comparisons were followed by a post-hoc test (Duncan's). Data are shown as mean ± SE obtained from 6 repeated experiments. TRPV1 phosphorylation at serine and threonine residues was assessed using 6 cultures each of which were generated from 2 rats. A total of 24 rats were used to complete these immunoprecipitation experiments.

3. Results

3.1 $P2X_3$-induced masseter hyperalgesia

Intramuscular injection of αβmeATP induced a dose- and time-dependent mechanical hyperalgesia (Fig. 1). Specifically, the two highest doses of αβmeATP, 500 and 750 μg, induced significant mechanical hyperalgesia (Drug: $F = 33.251$, $P < 0.001$; Fig. 1A). Hyperalgesia was observed at 15, 30 and 45 min post injection, with mechanical thresholds returning to baseline by 60 min (Time: $F = 66.046$, $P < 0.001$, Fig. 1A). In order to examine the overall magnitude of drug effect irrespective of time, AUC was calculated for the normalized data for each rat. Both 500 and 750 μg of αβmeATP induced significant mechanical hyperalgesia compared to PBS ($F = 34.701$, $P < 0.001$, Fig. 1B). The dose of 750 μg of αβmeATP was used throughout the remainder of this study.

The Von Frey (VF) anesthesiometer was applied to the masseter through the overlying skin. Therefore, similar to experiments performed previously (Ro et al., 2009), the overlying skin was anesthetized with a 20% benzocaine gel to confirm changes in mechanical sensitivity resulted from activation of muscular afferents. Intramuscular injections of αβmeATP induced a mechanical hyperalgesia that was not significantly different between animals with and without anesthetized skin, as shown by the AUC ($t = 0.274$, $P = 0.790$, Fig. 1C). The efficacy of the anesthetic was confirmed with a known algesic, capsaicin. The same concentration of benzocaine completely prevented intradermal capsaicin-induced nocifensive hindpaw shaking behavior, a behavior that lasted 45 min in the absence of benzocaine. A separate group of animals was tested to rule out the possibility that a high dose of αβmeATP (750 μg) could induce systemic effects. Mechanical sensitivity was tested in the muscle contralateral to the αβmeATP injection. The AUC was significantly different from the ipsilateral masseter which suggests the αβmeATP effect was mediated by local $P2X_3$ receptors ($t = -11.977$, $P < 0.001$, Fig. 1D). In order to confirm the specificity of

αβmeATP, we pretreated the masseter with the selective $P2X_3$ antagonist A-317491 (Jarvis et al., 2002; Wu et al., 2004). A-317491 dose-dependently blocked the effects of αβmeATP ($F = 46.690$, $P < 0.001$, Fig. 1E). In conclusion, αβmeATP induces a local $P2X_3$ mediated masseter mechanical hyperaglesia.

3.2 TRPV1 mediates $P2X_3$- induced masseter hyperalgesia

To determine if TRPV1 are involved in $P2X_3$-induced masseter hyperalgesia, animals were treated with a TRPV1 antagonist, AMG9810, prior to αβmeATP in the same muscle. AMG9810 dose-dependently prevented $P2X_3$-induced masseter hyperalgesia (Drug: $F = 43.106$, $P < 0.001$, Fig. 2A). Mechanical hyperalgesia was observed at 15, 30, and 45 min (Time: $F = 170.503$, $P < 0.001$, Fig. 2A). In order to assess the overall magnitude of drug effect irrespective of time a one-way ANOVA was performed on the AUC. AMG9810 significantly prevented αβmeATP-induced mechanical hyperalgesia compared to vehicle ($F = 54.797$, $P < 0.001$, Fig. 2B). When the highest dose of AMG9810 (100 nmol) or DMSO was given alone there was no significant drug effect ($F = 2.619$, $P = 0.137$, Fig. 2C). While there was a slight but significant elevation of the mechanical sensitivity over time neither AMG9810 nor DMSO altered mechanical thresholds at earlier time points during which αβmeATP effects are prominent (Fig. 2C). Mechanical hyperalgesia was generally resolved by these later time points (Fig. 1A) and 10 nmol AMG9810, a 10-fold lower dose, significantly prevented αβmeATP effects (Fig. 2A).

To exclude the possibility that AMG9810 directly suppresses $P2X_3$, we examined the effects of AMG9810 on αβmeATP responses. Since it is difficult to assess the nonspecific effects of AMG9810 on $P2X_3$ *in vivo*, we examined Ca^{2+} responses in TG cultures by performing ratiometric Ca^{2+} imaging. We evaluated the neuronal responses evoked by αβmeATP (50 μM) following pretreatment and co-application with either AMG9810 (1 μM) or vehicle (Fig. 3A). This protocol was tested on 2 cultures generated from 2 rats. There was no significant difference in the amplitude of αβmeATP–evoked responses between AMG9810 and vehicle treated neurons (AMG9810 = 0.51 ± 0.06, vehicle = 0.42 ± 0.03, $P = 0.96$, Mann-Whitney test, Fig. 3B). The proportions of the responding neurons were not significantly different either [vehicle, 27% (62/225); AMG9810, 24% (44/182); $P = 0.58$, Fisher's exact test]. These results suggest that AMG9810 did not directly suppress $P2X_3$ in the behavioral experiments.

3.3 Co-expression of TRPV1 and $P2X_3$ in masseter afferents

Although co-expression of $P2X_3$ and TRPV1 has been demonstrated in TG neurons (Eriksson et al., 1998; Ichikawa et al., 2004; Ichikawa and Sugimoto, 2004; Kim et al., 2011), to our knowledge co-expression in masseter afferents has not been reported. To establish a cellular basis for the functional interaction observed between $P2X_3$ and TRPV1 we sought to confirm co-expression of these channels in masseter afferents. The expression profile of TRPV1 and $P2X_3$ was assessed in 400 masseter afferents. The retrograde labeling of masseter afferents by Fast Blue (FB) was limited to the mandibular division of TG. TRPV1 were observed in predominantly small to medium sized neurons (Fig. 4A). While $P2X_3$ were expressed in all sized cells they were predominant in medium sized neurons (Fig. 4A). Specifically, TRPV1 were expressed in 34.6 ± 5.3% in masseter afferents and $P2X_3$

29.5 ± 7.2% (Fig 4B). TRPV1 and $P2X_3$ were co-expressed in 7.2 ± 3.1% of masseter afferents, with a mean soma size of 646.2 ± 59.7μm^2 (Fig. 4B).

3.4 $P2X_3$ sensitizes TRPV1 Ca^{2+} transients

To assess the $P2X_3$-TRPV1 interaction at the cellular level we utilized the following protocol in conjunction with the Ca^{2+} imaging technique. Depicted in Fig. 5A and 5B, an initial sub-maximal concentration of capsaicin (10 nM) was applied to assess the basal responses across individual cells and TG culture preparations. Ten minutes later, vehicle in the control group or αβmeATP in the experimental group was applied for 1 min. Following the vehicle or αβmeATP application, a second application of 10 nM capsaicin was made. A sub-maximal concentration of capsaicin was used to minimize the desensitizing effects of repeated capsaicin applications, and also to ensure that sensitization can be clearly observed while ceiling effects are avoided. In the control condition, after the second 10 nM capsaicin application αβmeATP was applied to identify $P2X_3$ receptor positive cells. At the end of the experiment, a supramaximal concentration of capsaicin (1 μM) was applied to confirm the identification of all TRPV1 neurons in both experimental and control conditions.

The proportion of capsaicin responsive neurons that responded to αβmeATP was the same across conditions (Table 1). The proportion of αβmeATP responsive neurons that responded to capsaicin was also similar across conditions (Table 1). In our analysis we included only neurons that responded to both capsaicin and αβmeATP (experimental = 217 and control = 180). In order to determine the effect of $P2X_3$ activation on TRPV1 activity, we compared capsaicin-induced Ca^{2+} transients following treatment with either vehicle or 50 μM αβmeATP (Fig. 5A,B). We observed two types of responses; some neurons exhibited decreased responses to the second capsaicin treatment (desensitization) while others displayed increased responses (sensitization). The proportion of neurons showing desensitizing and sensitizing responses was similar in control and experimental groups (Table 1).

In the desensitizing subset of neurons, the magnitude of the second capsaicin-evoked response was significantly smaller compared to the first (Time: $F = 72.573$, $P < 0.001$). This desensitization occurred to the same extent in both control and αβmeATP treated neurons (Drug: $F = 1.193$, $P = 0.276$; $\Delta FR_{experimental}$, $1^{St} = 0.28 \pm 0.04$, $2^{nd} = 0.08 \pm 0.02$; $\Delta FR_{control}$, $1^{St} = 0.21 \pm 0.30$, $2^{nd} = 0.07 \pm 0.01$). In the sensitizing subset of neurons, however, αβmeATP treatment evoked a significantly greater increase in Ca^{2+} influx compared to vehicle (Drug: $F = 8.672$, $P = 0.004$; Time: $F = 18.632$, $P < 0.001$, Fig. 5C). Furthermore, cells exhibiting desensitizing behavior typically showed a larger Ca^{2+} influx during the initial capsaicin application whereas the cells exhibiting sensitizing responses tended to have initially smaller Ca^{2+} responses regardless of treatment group (Desensitizing: $\Delta FR_{experimental}$ $1^{St} = 0.28 \pm 0.04$, $\Delta FR_{control}$ $1^{S} = 0.21 \pm 0.30$; Sensitizing: $\Delta FR_{experimental}$ $1^{St} = 0.06 \pm 0.01$, $\Delta FR_{control}$ $1^{St} = 0.04 \pm 0.01$). This suggests that $P2X_3$ activation potentiates the sensitization of TRPV1 responses in this subset of TG neurons.

Since αβmeATP can activate $P2X_3$ as well as $P2X_1$ receptors (Torres et al., 1998; North and Surprenant, 2000), it is possible that a portion of the αβmeATP effects in our experiments could be mediated by $P2X_1$. To exclude this possibility, we tested the effects of the selective

$P2X_3$ antagonist A-317491 ((Jarvis et al., 2002), 500 nM, 1 μM, 3 μM) on the effects of αβmeATP (50 μM). We saw a significant dose-dependent reduction in the percentage of responsive neurons ($P < 0.001$, Fig. 6A) and the amplitude of αβmeATP-evoked Ca^{2+} transients ($P < 0.001$, Fig. 6B). These data suggest that the αβmeATP effects we observed are mediated primarily by $P2X_3$.

3.5 $P2X_3$ induces phosphorylation of TRPV1 at specific residues

As another measure of $P2X_3$-TRPV1 interactions we investigated whether activation of $P2X_3$ induces phosphorylation of TRPV1. It is not feasible to test phosphorylation at the primary afferent terminal level since the neural elements in the muscle tissue are too low to detect meaningful biochemical changes. Therefore, we assessed the relative level of TRPV1 phosphorylation in TG cultures 15, 30, and 45 min following the application of αβmeATP (50 μM). The application of αβmeATP caused a time-dependent increase in serine phosphorylation (p-Ser) of TRPV1 (Fig. 7A and B). This increase peaks 15 to 30 min after the application, however, it only reached significance at 15 min. Interestingly, the mechanical hyperalgesia which develops following αβmeATP injection in the *in vivo* condition was most prominent during the same time period. The same concentration of αβmeATP did not induce significant changes in the phosphorylation of TRPV1 at threonine residues (Fig. 7C and D). As a control for phosphorylation, we have treated TG cultures with either the PKC activator PMA or vehicle (0 or 15 min). PKC is known to phosphorylate serine residues on TRPV1 (Numazaki et al., 2002; Bhave et al., 2003; Mandadi et al., 2006). PMA (1μmol) produced increased phosphorylated serine compared to vehicle and no treatment (Fig. 8). Additional experiments were also completed using the western blot technique to assess whether there were any changes in the levels of TRPV1 expression 15, 30, and 45 min following the application of αβmeATP (50μM). There were no significant differences in TRPV1 expression (Fig. 9). These data provide support for $P2X_3$-TRPV1 interactions and that $P2X_3$ activation leads to TRPV1 phosphorylation at specific sites.

4. Discussion

This study demonstrated a functional interaction between $P2X_3$ and TRPV1, which contributes to the development of masseter mechanical hyperalgesia. First, we validated that muscular $P2X_3$ activation induces mechanical hyperaglesia with our own orofacial model. Second, we demonstrated that $P2X_3$-induced mechanical hyperaglesia is mediated by TRPV1. Next, we determined that TRPV1 and $P2X_3$ are expressed in a subpopulation of masseter afferents. Fourth, we illustrated that $P2X_3$ activation enhances capsaicin-induced responses in a subset of TG neurons. Finally, we reported $P2X_3$ activation induces residue specific phosphorylation of TRPV1 in sensory neurons at time points in which mechanical hyperalgesia was observed. These data provide novel information suggesting the interaction between two ligand-gated channels, $P2X_3$ and TRPV1, contributes to the development of muscle mechanical hyperalgesia.

The $P2X_3$ type ATP receptors are unique nociceptive targets because they are expressed almost exclusively in peripheral sensory neurons (Chen et al., 1995; Bradbury et al., 1998; Dunn et al., 2001). $P2X_3$ were previously implicated in masseter hyperalgesia. αβmeATP

injected into the masseter induced a mechanical hyperalgesia that was blocked by the non-specific antagonist PPADS (Shinoda et al., 2008). Here, we replicated αβmeATP-induced masseter hyperalgesia in another orofacial muscle pain model. In both models, no hyperalgesia was observed in the masseter contralateral to the αβmeATP injection suggesting a peripheral mechanism of action. We validated the effect with a specific $P2X_3$ antagonist confirming it is $P2X_3$-mediated. Our benzocaine control experiments confirmed the αβmeATP effect is mediated by $P2X_3$ innervating muscle. Together, our data suggest local $P2X_3$ are mediating masseter mechanical hyperalgesia. In humans, ATP infusion during capsaicin application significantly enhances touch-evoked hyperalgesia (Hamilton et al., 2000) suggesting a facilitatory interaction between purinoceptors and TRPV1. In our data, $P2X_3$-induced masseter hyperalgesia was prevented by TRPV1 blockade supporting the notion that $P2X_3$ and TRPV1 interact in a facilitatory manner.

Previously, there was little to no information available regarding the extent and pattern of co-expression in muscle afferents between $P2X_3$ and TRPV1. Immunohistochemistry studies reported approximately 33–58% of all TG neurons co-express $P2X_3$ and TRPV1 (Eriksson et al., 1998; Ichikawa et al., 2004; Ichikawa and Sugimoto, 2004). More recently, the expression pattern of $P2X_3$ and TRPV1 in masseter afferents have been looked at independently of each other. Specifically, 22% and 24–38% of masseter afferents express $P2X_3$ and TRPV1, respectively (Ambalavanar et al., 2005; Takeda et al., 2005; Simonetti et al., 2006; Staikopoulos et al., 2007; Ro et al., 2009). We observed percentages of $P2X_3$ (29.5 ± 7.2%) and TRPV1 (34.6 ± 5.3%) immunoreactive masseter afferents consistent with the current literature, and that 7.2 ± 3.1% medium-sized afferents co-express $P2X_3$ and TRPV1. To our knowledge this is the first report of the co-expression pattern of these two channels in masseter afferents.

There is an apparent discrepancy between the small proportion of masseter afferents co-expressing TRPV1 and $P2X_3$ and the robust behavioral phenotype. This disparity could be attributed to a variety of factors. There is precedence for a specific but small population of receptor-specific neurons producing robust physiological effects. For instance, TRPM8, which is expressed in only 5–10% of DRG neurons (Reid and Flonta, 2001; McKemy et al., 2002; Peier et al., 2002) mediate cold sensation in the range of 22–27°C (Peier et al., 2002; Bautista et al., 2007). TRPM8 null mice exhibit an array of deficits including a reduction in avoidance of cold zones, increased response latencies to the cold plate test, and reduced responses to acetone (Bautista et al., 2007; Colburn et al., 2007; Dhaka et al., 2007). Similarly, MrgprA3 which is the major receptor responsible for chloroquine (CQ)-induced itch, is expressed in only 4–5% of DRG neurons (Liu et al., 2009). *Mrgpr-cluster* $\Delta^{-/-}$ mice have ~30 *Mrgpr* genes deleted and they exhibit a significant reduction in CQ-induced scratching behavior (Liu et al., 2009). *Mrgpr-cluster* $\Delta^{-/-}$ DRG display a considerably reduced Ca^{2+} response to CQ, which is rescued by MrgprA3 expression.

Furthermore, pathophysiological manipulations such as masseter or TMJ inflammation, masseter stretching or eccentric contraction, as well as tooth movement significantly increase $P2X_3$ expression in TG for several days (Ambalavanar et al., 2005; Shinoda et al., 2005; Yang et al., 2009; Dessem et al., 2010). Thus, it is likely that under clinical or

injurious conditions the extent of co-expression between these channels increases, providing a greater opportunity for these channels to interact.

Moreover, during an inflammatory event, mediators are released that can modulate TRPV1, further enhancing the observed behavioral effects. Thus, as opposed to a reduced *in vitro* preparation, other signaling sources could be present *in vivo*. In the case of this study, it is possible that the mechanical stimulation or cation channel activation, particularly TRPV1, induced the activation of mast cells (Turner et al., 2007). Degranulation of mast cells induces release of a protease, tryptase, which is known to sensitize TRPV1 (Amadesi, 2004). Although additional sensitization of TRPV1 by resident modulators could enhance the effects of $P2X_3$ *in vivo*, our behavioral and cellular data still support the notion that $P2X_3$ contributes to a facilitatory interaction with TRPV1.

When we applied a submaximal concentration of capsaicin (10 nM) repeatedly in the Ca^{2+} imaging experiments, we observed desensitizing effects in ~65% of neurons. αβmeATP treatment did not alter the extent of desensitization in this population. When we focused our analysis on the 35% of neurons that do not undergo desensitization, we discovered the sensitizing effects of αβmeATP.

We believe the desensitizing effect is reflective of the classical Ca^{2+}-dependent desensitization that typically occurs following repeated application of capsaicin (Cholewinski et al., 1993; Docherty et al., 1996; Koplas et al., 1997). It is unclear whether the $P2X_3$-TRPV1 interaction also exists in this population. It is possible that the intracellular machineries necessary for functional interactions between the two channels are absent or not operational in this subset of neurons. Alternatively, it is possible that capsaicin-induced desensitization is too strong to reveal the modest sensitizing effect of αβmeATP. It has been shown that desensitization/sensitization of TRPV1 is dependent on the initial concentration of Ca^{2+} influx in DRG (Zhang et al., 2011). Thus, within the heterogeneous population co-expressing TRPV1 and $P2X_3$, there is a subset of neurons that have the capability of being sensitized by αβmeATP. Differences in initial TRPV1 responses may confer the identity of neurons as sensitizers or desensitizers. The sources of heterogeneity of initial TRPV1 responses within the general TRPV1/$P2X_3$ population could result from basal differences in expression level or phosphorylation state of TRPV1, which requires further investigation.

Our data demonstrates phosphorylation and sensitization of TRPV1 following pretreatment with αβmeATP. However, activation of $P2X_3$ can lead to Ca^{2+} influx, which in turn facilitates desensitization of TRPV1. Such Ca^{2+}-dependent inhibitory interactions between $P2X_3$ and TRPV1 were reported in a heterologous system as well as in sensory neurons (Piper and Docherty, 2000; Stanchev et al., 2009). In our experiments, we applied a low concentration of capsaicin (10 nM) in which approximately 35% of neurons did not undergo desensitization upon repeated application. However, in the case of applying higher capsaicin concentrations (e.g., 10 μM), as adopted in previous studies (Piper and Docherty, 2000; Stanchev et al., 2009), the population of neurons displaying desensitization would be predominant and hence sensitizing interactions would hardly be observed. Thus, physiologically we presume that both potentiating and inhibiting interactions between $P2X_3$ and TRPV1 could occur in nociceptors, and that the consequence of the interactions could

be dependent on multiple factors such as the extent of initial activation and kinase availability. Further examination of cellular mechanisms underlying dynamic interactions between $P2X_3$ and TRPV1 is warranted.

Increased TRPV1 function, sensitization, is well documented. One of the mechanisms through which such potentiation of TRPV1 function occurs is phosphorylation events (Bhave et al., 2002; Bhave et al., 2003; Jung et al., 2004; Mandadi et al., 2006; Jeske et al., 2008; Woo et al., 2008; Jeske et al., 2009). For example, PKC targets Ser-800, Ser-502, Thr-704, and Thr-144 on TRPV1 (Numazaki et al., 2002; Bhave et al., 2003; Mandadi et al., 2006). CaMKII, on the other hand, targets Ser-502 and Thr-704 (Jung et al., 2004). Our data shows $P2X_3$-induced TRPV1 serine phosphorylation at the time point in which we observed peak hyperaglesia *in vivo*. Our data suggests distinct kinases may be involved in the $P2X_3$-TRPV1 interaction.

It is well established that GPCRs form ‘functional units’ with TRPV1 (Levine and Alessandri-Haber, 2007), but now there are data emerging to suggest ligand-gated channels form ‘functional units’ as well. Both glutamate and ATP are mediators released in high concentrations during injury and inflammation. Their receptors, $P2X_3$ and NMDA receptor (NMDAR), are nonselective cation channels co-expressed with TRPV1 in masseter afferents. Similar to our data, direct activation of NMDARs induces a masseter hyperalgesia that is prevented by treatment with a TRPV1 antagonist (Lee et al., 2012). Akin to $P2X_3$ activation, NMDAR activation induces phosphorylation of only serine residues on TRPV1. Recently, we also demonstrated that NMDARs functionally interact with TRPV1 in a CaMKII- and PKC-dependent manner (Lee et al., 2011; Lee et al., 2012). TRPV1 is known to be phosphorylated and sensitized by CaMKII and PKC (Premkumar and Ahern, 2000; Bhave et al., 2003; Jung et al., 2004; Woo et al., 2008). ATP receptors, including $P2X_3$, have been linked to CaMKII and PKC kinase activation (Tominaga et al., 2001; Han et al., 2008). It will be interesting to determine whether these two cation channels interact via these Ca^{2+}-dependent kinases.

5. Conclusions

This study identifies a new interaction, $P2X_3$-TRPV1 in trigeminal sensory neurons, which could contribute to the development of mechanical hyperalgesia. In light of a recent study that showed the role of $P2X_5$-ASIC3 interaction in muscle afferents under muscle ischemia condition (Birdsong et al., 2010) our data reinforces the notion that channel-channel interactions in sensory neurons provide mechanisms by which nociceptor function is dynamically modulated. TMD patients often suffer from mechanical hyperalgesia of masticatory musculature (Harness et al., 1990; Stohler, 1999). Unfortunately, currently available pharmacological interventions are often ineffective and produce undesirable side effects (Cowan et al., 1988; Sheldon et al., 1990; Cheng et al., 1993). Further elucidating these peripheral mechanisms could lead to the advent of more targeted and effective therapeutics for pain management that are unaccompanied by such unwanted side effects.

Acknowledgments

The authors thank Gregory Haynes for technical assistance performing behavioral experiments. This study was supported by NIH grants F31 DE20966 to JLS, DE020866 to MKC, and RO1 DE16062 to JYR.

Abbreviations

αβmeATP	alpha,beta-methylene adenosine triphosphate
AUC	area under the curve
CIB	calcium imaging buffer
CQ	chloroquine
DRG	dorsal root ganglia
GPCR	G-protein coupled receptor
FR	Fura Response
FB	fast blue
KO	knockout
LDS	lithium dodecyl sulfate
NMDAR	NMDA receptor
TMJ	temporomandibular joint
TMD	temporomandibular joint and muscle disorder
TRPV1	transient receptor potential V1
TG	trigminal ganglia
SDS	Sodium dodecyl sulfate
p-Ser	serine phosphorylation
SE	standard error of the mean
VF	von frey

References

Ambalavanar R, Moritani M, Dessem D. Trigeminal P2X3 receptor expression differs from dorsal root ganglion and is modulated by deep tissue inflammation. Pain. 2005; 117:280–291. [PubMed: 16153775]

Arendt-Nielsen L, Svensson P, Sessle BJ, Cairns BE, Wang K. Interactions between glutamate and capsaicin in inducing muscle pain and sensitization in humans. European Journal of Pain: Ejp. 2008; 12:661–670.

Bautista DM, Siemens J, Glazer JM, Tsuruda PR, Basbaum AI, Stucky CL, Jordt SE, Julius D. The menthol receptor TRPM8 is the principal detector of environmental cold. Nature. 2007; 448:204–208. [PubMed: 17538622]

Bhave G, Zhu W, Wang H, Brasier DJ, Oxford GS, Gereau RWt. cAMP-dependent protein kinase regulates desensitization of the capsaicin receptor (VR1) by direct phosphorylation. Neuron. 2002; 35:721–731. [PubMed: 12194871]

Bhave G, Hu HJ, Glauner KS, Zhu W, Wang H, Brasier DJ, Oxford GS, Gereau RWt. Protein kinase C phosphorylation sensitizes but does not activate the capsaicin receptor transient receptor potential vanilloid 1 (TRPV1) . Proceedings of the National Academy of Sciences of the United States of America. 2003; 100:12480–12485. [PubMed: 14523239]

Birdsong WT, Fierro L, Williams FG, Spelta V, Naves LA, Knowles M, Marsh-Haffner J, Adelman JP, Almers W, Elde RP, McCleskey EW. Sensing Muscle Ischemia: Coincident Detection of Acid and ATP via Interplay of Two Ion Channels. Neuron. 2010; 68:739–749. [PubMed: 21092862]

Bradbury EJ, Burnstock G, McMahon SB. The expression of P2X3 purinoreceptors in sensory neurons: effects of axotomy and glial-derived neurotrophic factor. Molecular & Cellular Neurosciences. 1998; 12:256–268. [PubMed: 9828090]

Chen CC, Akopian AN, Sivilotti L, Colquhoun D, Burnstock G, Wood JN. A P2X purinoceptor expressed by a subset of sensory neurons. Nature. 1995; 377:428–431. [PubMed: 7566119]

Cheng PY, Wu D, Decena J, Soong Y, McCabe S, Szeto HH. Opioid-induced stimulation of fetal respiratory activity by [D-Ala2]deltorphin I. European journal of pharmacology. 1993; 230:85–88. [PubMed: 8381356]

Cholewinski A, Burgess GM, Bevan S. The role of calcium in capsaicin-induced desensitization in rat cultured dorsal root ganglion neurons. Neuroscience. 1993; 55:1015–1023. [PubMed: 7694175]

Chun YH, Frank D, Lee JS, Zhang Y, Auh QS, Ro JY. Peripheral AMPA receptors contribute to muscle nociception and c-fos activation. Neuroscience research. 2008; 62:97–104. [PubMed: 18655811]

Colburn RW, Lubin ML, Stone DJ Jr, Wang Y, Lawrence D, D'Andrea MichaelÂ R, Brandt MR, Liu Y, Flores CM, Qin N. Attenuated Cold Sensitivity in TRPM8 Null Mice. Neuron. 2007; 54:379–386. [PubMed: 17481392]

Cowan A, Zhu XZ, Mosberg HI, Omnaas JR, Porreca F. Direct dependence studies in rats with agents selective for different types of opioid receptor. Journal of Pharmacology & Experimental Therapeutics. 1988; 246:950–955. [PubMed: 2901490]

Dessem D, Ambalavanar R, Evancho M, Moutanni A, Yallampalli C, Bai G. Eccentric muscle contraction and stretching evoke mechanical hyperalgesia and modulate CGRP and P2X3 expression in a functionally relevant manner. PAIN. 2010; 149:284–295. [PubMed: 20207080]

Dhaka A, Murray AN, Mathur J, Earley TJ, Petrus MJ, Patapoutian A. TRPM8 Is Required for Cold Sensation in Mice. Neuron. 2007; 54:371–378. [PubMed: 17481391]

Docherty R, Yeats J, Bevan S, Boddeke H. Inhibition of calcineurin inhibits the desensitization of capsaicin-evoked currents in cultured dorsal root ganglion neurones from adult rats. Pflugers Archiv European Journal of Physiology. 1996; 431:828–837. [PubMed: 8927498]

Dunn PM, Zhong Y, Burnstock G. P2X receptors in peripheral neurons. Progress in neurobiology. 2001; 65:107–134. [PubMed: 11403876]

Eriksson J, Bongenhielm U, Kidd E, Matthews B, Fried K. Distribution of P2X3 receptors in the rat trigeminal ganglion after inferior alveolar nerve injury. Neuroscience Letters. 1998; 254:37–40. [PubMed: 9780086]

Fujii Y, Ozaki N, Taguchi T, Mizumura K, Furukawa K, Sugiura Y. TRP channels and ASICs mediate mechanical hyperalgesia in models of inflammatory muscle pain and delayed onset muscle soreness. Pain. 2008; 140:292–304. [PubMed: 18834667]

Guo A, Vulchanova L, Wang J, Li X, Elde R. Immunocytochemical localization of the vanilloid receptor 1 (VR1): relationship to neuropeptides, the P2X3 purinoceptor and IB4 binding sites. European Journal of Neuroscience. 1999; 11:946–958. [PubMed: 10103088]

Hamilton SG, Warburton J, Bhattacharjee A, Ward J, McMahon SB. ATP in human skin elicits a dose-related pain response which is potentiated under conditions of hyperalgesia. Brain. 2000; 123:1238–1246. [PubMed: 10825361]

Han SR, Lee MK, Lim KH, Yang GY, Jeon HJ, Ju JS, Yoon YW, Kim SK, Ahn DK. Intramuscular administration of morphine reduces mustard-oil-induced craniofacial-muscle pain behavior in lightly anesthetized rats. European Journal of Pain: Ejp. 2008; 12:361–370.

Harness DM, Donlon WC, Eversole LR. Comparison of clinical characteristics in myogenic, TMJ internal derangement and atypical facial pain patients. Clinical Journal of Pain. 1990; 6:4–17. [PubMed: 2134994]

Hasegawa S, Kohro Y, Tsuda M, Inoue K. Activation of cytosolic phospholipase A2 in dorsal root ganglion neurons by Ca2+/calmodulin-dependent protein kinase II after peripheral nerve injury. Molecular pain. 2009; 5:22. [PubMed: 19409102]

Hoheisel U, Reinohl J, Unger T, Mense S. Acidic pH and capsaicin activate mechanosensitive group IV muscle receptors in the rat. Pain. 2004; 110:149–157. [PubMed: 15275762]

Honore P, Wismer CT, Mikusa J, Zhu CZ, Zhong C, Gauvin DM, Gomtsyan A, El Kouhen R, Lee CH, Marsh K, Sullivan JP, Faltynek CR, Jarvis MF. A-425619 [1-isoquinolin-5-yl-3-(4-trifluoromethyl-benzyl)-urea], a novel transient receptor potential type V1 receptor antagonist, relieves pathophysiological pain associated with inflammation and tissue injury in rats. Journal of Pharmacology & Experimental Therapeutics. 2005; 314:410–421. [PubMed: 15837818]

Ichikawa H, Sugimoto T. The co-expression of P2X3 receptor with VR1 and VRL-1 in the rat trigeminal ganglion. Brain research. 2004; 998:130–135. [PubMed: 14725976]

Ichikawa H, Fukunaga T, Jin HW, Fujita M, Takano-Yamamoto T, Sugimoto T. VR1-, VRL-1- and P2X3 receptor-immunoreactive innervation of the rat temporomandibular joint. Brain research. 2004; 1008:131–136. [PubMed: 15081392]

Jarvis MF, Burgard EC, McGaraughty S, Honore P, Lynch K, Brennan TJ, Subieta A, Van Biesen T, Cartmell J, Bianchi B, Niforatos W, Kage K, Yu H, Mikusa J, Wismer CT, Zhu CZ, Chu K, Lee CH, Stewart AO, Polakowski J, Cox BF, Kowaluk E, Williams M, Sullivan J, Faltynek C. A-317491, a novel potent and selective non-nucleotide antagonist of P2X3 and P2X2/3 receptors, reduces chronic inflammatory and neuropathic pain in the rat. Proceedings of the National Academy of Sciences of the United States of America. 2002; 99:17179–17184. [PubMed: 12482951]

Jeske NA, Patwardhan AM, Ruparel NB, Akopian AN, Shapiro MS, Henry MA. A-kinase anchoring protein 150 controls protein kinase C-mediated phosphorylation and sensitization of TRPV1. PAIN. 2009; 146:301–307. [PubMed: 19767149]

Jeske NA, Diogenes A, Ruparel NB, Fehrenbacher JC, Henry M, Akopian AN, Hargreaves KM. A-kinase anchoring protein mediates TRPV1 thermal hyperalgesia through PKA phosphorylation of TRPV1. Pain. 2008; 138:604–616. [PubMed: 18381233]

Jung J, Shin JS, Lee SY, Hwang SW, Koo J, Cho H, Oh U. Phosphorylation of vanilloid receptor 1 by Ca2+/calmodulin-dependent kinase II regulates its vanilloid binding. Journal of Biological Chemistry. 2004; 279:7048–7054. [PubMed: 14630912]

Kim HY, Chung G, Jo HJ, Kim YS, Bae YC, Jung SJ, Kim JS, Oh SB. Characterization of Dental Nociceptive Neurons. Journal of Dental Research. 2011; 90:771–776. [PubMed: 21364091]

Kim YS, Paik SK, Cho YS, Shin HS, Bae JY, Moritani M, Yoshida A, Ahn DK, Valtschanoff J, Hwang SJ, Moon C, Bae YC. Expression of P2X3 receptor in the trigeminal sensory nuclei of the rat. The Journal of Comparative Neurology. 2008; 506:627–639. [PubMed: 18067147]

Koplas PA, Rosenberg RL, Oxford GS. The Role of Calcium in the Desensitization of Capsaicin Responses in Rat Dorsal Root Ganglion Neurons. The Journal of Neuroscience. 1997; 17:3525–3537. [PubMed: 9133377]

Lee J, Saloman JL, Weiland G, Auh QS, Chung M-K, Ro JY. Functional interactions between NMDA receptors and TRPV1 in trigeminal sensory neurons mediate mechanical hyperalgesia in the rat masseter muscle. PAIN. 2012; 153:1514–1524. [PubMed: 22609428]

Lee, JS.; Zhang, Y.; Chung, MK.; Ro, JY. Society for Neuroscience. Washington, D.C.: 2011. Protein Kinase C and AKAP150 are involved in functional interactions between NMDA receptors and TRPV1 in trigeminal ganglia.

Levine JD, Alessandri-Haber N. TRP channels: targets for the relief of pain. Biochimica et biophysica acta. 2007; 1772:989–1003. [PubMed: 17321113]

Liu Q, Tang Z, Surdenikova L, Kim S, Patel KN, Kim A, Ru F, Guan Y, Weng H-J, Geng Y, Undem BJ, Kollarik M, Chen Z-F, Anderson DJ, Dong X. Sensory Neuron-Specific GPCR Mrgprs Are Itch Receptors Mediating Chloroquine-Induced Pruritus. Cell. 2009; 139:1353–1365. [PubMed: 20004959]

Malin SA, Davis BM, Koerber HR, Reynolds IJ, Albers KM, Molliver DC. Thermal nociception and TRPV1 function are attenuated in mice lacking the nucleotide receptor P2Y2. Pain. 2008; 138:484–496. [PubMed: 18343036]

Mandadi S, Tominaga T, Numazaki M, Murayama N, Saito N, Armati PJ, Roufogalis BD, Tominaga M. Increased sensitivity of desensitized TRPV1 by PMA occurs through PKCepsilon-mediated phosphorylation at S800. Pain. 2006; 123:106–116. [PubMed: 16564619]

McKemy DD, Neuhausser WM, Julius D. Identification of a cold receptor reveals a general role for TRP channels in thermosensation. Nature. 2002; 416:52–58. [PubMed: 11882888]

Moriyama T, Iida T, Kobayashi K, Higashi T, Fukuoka T, Tsumura H, Leon C, Suzuki N, Inoue K, Gachet C, Noguchi K, Tominaga M. Possible involvement of P2Y2 metabotropic receptors in ATP-induced transient receptor potential vanilloid receptor 1-mediated thermal hypersensitivity. Journal of Neuroscience. 2003; 23:6058–6062. [PubMed: 12853424]

North RA, Surprenant A. Pharmacology of cloned P2X receptors. Annual Review of Pharmacology & Toxicology. 2000; 40:563–580.

Numazaki M, Tominaga T, Toyooka H, Tominaga M. Direct Phosphorylation of Capsaicin Receptor VR1 by Protein Kinase CÎµ and Identification of Two Target Serine Residues. Journal of Biological Chemistry. 2002; 277:13375–13378. [PubMed: 11884385]

Oliveira MC, Parada CA, Veiga MC, Rodrigues LR, Barros SP, Tambeli CH. Evidence for the involvement of endogenous ATP and P2X receptors in TMJ pain. European Journal of Pain: Ejp. 2005; 9:87–93.

Pabbidi R, Yu S-Q, Peng S, Khardori R, Pauza M, Premkumar L. Influence of TRPV1 on diabetes-induced alterations in thermal pain sensitivity. Molecular Pain. 2008; 4:9. [PubMed: 18312687]

Peier AM, Moqrich A, Hergarden AC, Reeve AJ, Andersson DA, Story GM, Earley TJ, Dragoni I, McIntyre P, Bevan S, Patapoutian A. A TRP Channel that Senses Cold Stimuli and Menthol. Cell. 2002; 108:705–715. [PubMed: 11893340]

Piper AS, Docherty RJ. One-way cross-desensitization between P2X purinoceptors and vanilloid receptors in adult rat dorsal root ganglion neurones. Journal of Physiology. 2000; 523:685–696. [PubMed: 10718747]

Pomonis JD, Harrison JE, Mark L, Bristol DR, Valenzano KJ, Walker K. N-(4-Tertiarybutylphenyl)-4-(3-cholorphyridin-2-yl)tetrahydropyrazine-1(2H)-carbox-amide (BCTC), a novel, orally effective vanilloid receptor 1 antagonist with analgesic properties: II. in vivo characterization in rat models of inflammatory and neuropathic pain. Journal of Pharmacology & Experimental Therapeutics. 2003; 306:387–393. [PubMed: 12721336]

Premkumar LS, Ahern GP. Induction of vanilloid receptor channel activity by protein kinase C. Nature. 2000; 408:985–990. [PubMed: 11140687]

Reid G, Flonta M-L. Physiology: Cold current in thermoreceptive neurons. Nature. 2001; 413:480–480. [PubMed: 11586349]

Reinohl J, Hoheisel U, Unger T, Mense S. Adenosine triphosphate as a stimulant for nociceptive and non-nociceptive muscle group IV receptors in the rat. Neuroscience letters. 2003; 338:25–28. [PubMed: 12565132]

Ro JY, Capra NF. Assessing mechanical sensitivity of masseter muscle in lightly anesthetized rats: a model for craniofacial muscle hyperalgesia. Neuroscience research. 2006; 56:119–123. [PubMed: 16857282]

Ro JY, Capra N, Masri R. Development of a behavioral assessment of craniofacial muscle pain in lightly anesthetized rats. Pain. 2003; 104:179–185. [PubMed: 12855327]

Ro JY, Lee JS, Zhang Y. Activation of TRPV1 and TRPA1 leads to muscle nociception and mechanical hyperalgesia. Pain. 2009; 144:270–277. [PubMed: 19464796]

Ro JY, Lee J, Capra NF, Zhang Y. Role of soluble guanylate cyclase in the trigeminal subnucleus caudalis in capsaicin-induced muscle hypersensitivity. Brain research. 2007; 1184:141–148. [PubMed: 17980861]

Ruparel NB, Patwardhan AM, Akopian AN, Hargreaves KM. Homologous and heterologous desensitization of capsaicin and mustard oil responses utilize different cellular pathways in nociceptors. Pain. 2008; 135:271–279. [PubMed: 17590514]

Saloman JL, Niu KY, Ro JY. Activation of peripheral delta-opioid receptors leads to anti-hyperalgesic responses in the masseter muscle of male and female rats. Neuroscience. 2011; 190:379–385. [PubMed: 21664434]

Sanchez EM, Bagues A, Martin MI. Contributions of peripheral and central opioid receptors to antinociception in rat muscle pain models. Pharmacology Biochemistry and Behavior. 2010; 96:488–495.

Sheldon RJ, Riviere PJ, Malarchik ME, Moseberg HI, Burks TF, Porreca F. Opioid regulation of mucosal ion transport in the mouse isolated jejunum. Journal of Pharmacology & Experimental Therapeutics. 1990; 253:144–151. [PubMed: 2329501]

Shinoda M, Ozaki N, Sugiura Y. Involvement of ATP and its receptors on nociception in rat model of masseter muscle pain. Pain. 2008; 134:148–157. [PubMed: 17521813]

Shinoda M, Ozaki N, Asai H, Nagamine K, Sugiura Y. Changes in P2X3 receptor expression in the trigeminal ganglion following monoarthritis of the temporomandibular joint in rats. Pain. 2005; 116:42–51. [PubMed: 15936887]

Simonetti M, Fabbro A, D'Arco M, Zweyer M, Nistri A, Giniatullin R, Fabbretti E. Comparison of P2X and TRPV1 receptors in ganglia or primary culture of trigeminal neurons and their modulation by NGF or serotonin. Molecular pain. 2006; 2:11. [PubMed: 16566843]

Staikopoulos V, Sessle BJ, Furness JB, Jennings EA. Localization of P2X2 and P2X3 receptors in rat trigeminal ganglion neurons. Neuroscience. 2007; 144:208–216. [PubMed: 17110047]

Stanchev D, Blosa M, Milius D, Gerevich Z, Rubini P, Schmalzing G, Eschrich K, Schaefer M, Wirkner K, Illes P. Cross-inhibition between native and recombinant TRPV1 and P2X(3) receptors. Pain. 2009; 143:26–36. [PubMed: 19223122]

Stohler CS. Muscle-related temporomandibular disorders. Journal of orofacial pain. 1999; 13:273–284. [PubMed: 10823041]

Takeda M, Tanimoto T, Ito M, Nasu M, Matsumoto S. Role of capsaicin-sensitive primary afferent inputs from the masseter muscle in the C1 spinal neurons responding to tooth-pulp stimulation in rats. Experimental Brain Research. 2005; 160:107–117. [PubMed: 15289965]

Tominaga M, Wada M, Masu M. Potentiation of capsaicin receptor activity by metabotropic ATP receptors as a possible mechanism for ATP-evoked pain and hyperalgesia. Proceedings of the National Academy of Sciences of the United States of America. 2001; 98:6951–6956. [PubMed: 11371611]

Torres GE, Haines WR, Egan TM, Voigt MM. Co-Expression of P2X1 and P2X5 Receptor Subunits Reveals a Novel ATP-Gated Ion Channel. Molecular Pharmacology. 1998; 54:989–993. [PubMed: 9855626]

Vulchanova L, Riedl MS, Shuster SJ, Buell G, Surprenant A, North RA, Elde R. Immunohistochemical study of the P2X2 and P2X3 receptor subunits in rat and monkey sensory neurons and their central terminals. Neuropharmacology. 1997; 36:1229–1242. [PubMed: 9364478]

Walker KM, Urban L, Medhurst SJ, Patel S, Panesar M, Fox AJ, McIntyre P. The VR1 antagonist capsazepine reverses mechanical hyperalgesia in models of inflammatory and neuropathic pain. Journal of Pharmacology & Experimental Therapeutics. 2003; 304:56–62. [PubMed: 12490575]

Wang S, Lee J, Ro JY, Chung MK. Warmth suppresses and desensitizes damage-sensing ion channel TRPA1. Molecular Pain. 2012; 8

Woo DH, Jung SJ, Zhu MH, Park CK, Kim YH, Oh SB, Lee CJ. Direct activation of transient receptor potential vanilloid 1(TRPV1) by diacylglycerol (DAG). Molecular Pain. 2008; 4:42. [PubMed: 18826653]

Wu G, Whiteside GT, Lee G, Nolan S, Niosi M, Pearson MS, Ilyin VI. A-317491, a selective P2X3/P2X2/3 receptor antagonist, reverses inflammatory mechanical hyperalgesia through action at peripheral receptors in rats. European journal of pharmacology. 2004; 504:45–53. [PubMed: 15507220]

Xu X, Wang P, Zou X, Li D, Fang L, Gong K, Lin Q. The effects of sympathetic outflow on upregulation of vanilloid receptors TRPV1 in primary afferent neurons evoked by intradermal capsaicin. Experimental Neurology. 2010; 222:93–107. [PubMed: 20036240]

Yang Z, Cao Y, Wang Y, Luo W, Hua X, Lu Y, Liao Z, Lai W, Zhao Z. Behavioural responses and expression of P2X3 receptor in trigeminal ganglion after experimental tooth movement in rats. Archives of Oral Biology. 2009; 54:63–70. [PubMed: 18945422]

Zhang X, Daugherty SL, de Groat WC. Activation of CaMKII and ERK1/2 contributes to the time-dependent potentiation of Ca2+ response elicited by repeated application of capsaicin in rat DRG neurons. American Journal of Physiology - Regulatory, Integrative and Comparative Physiology. 2011; 300:R644–R654.

Highlights

- $P2X_3$ induced mechanical hyperalgesia is attenuated by a TRPV1 antagonist
- A $P2X_3$ agonist potentiated capsaicin-induced Ca^{2+} transients in a subset of neurons
- $P2X_3$ activation induced serine phosphorylation of TRPV1

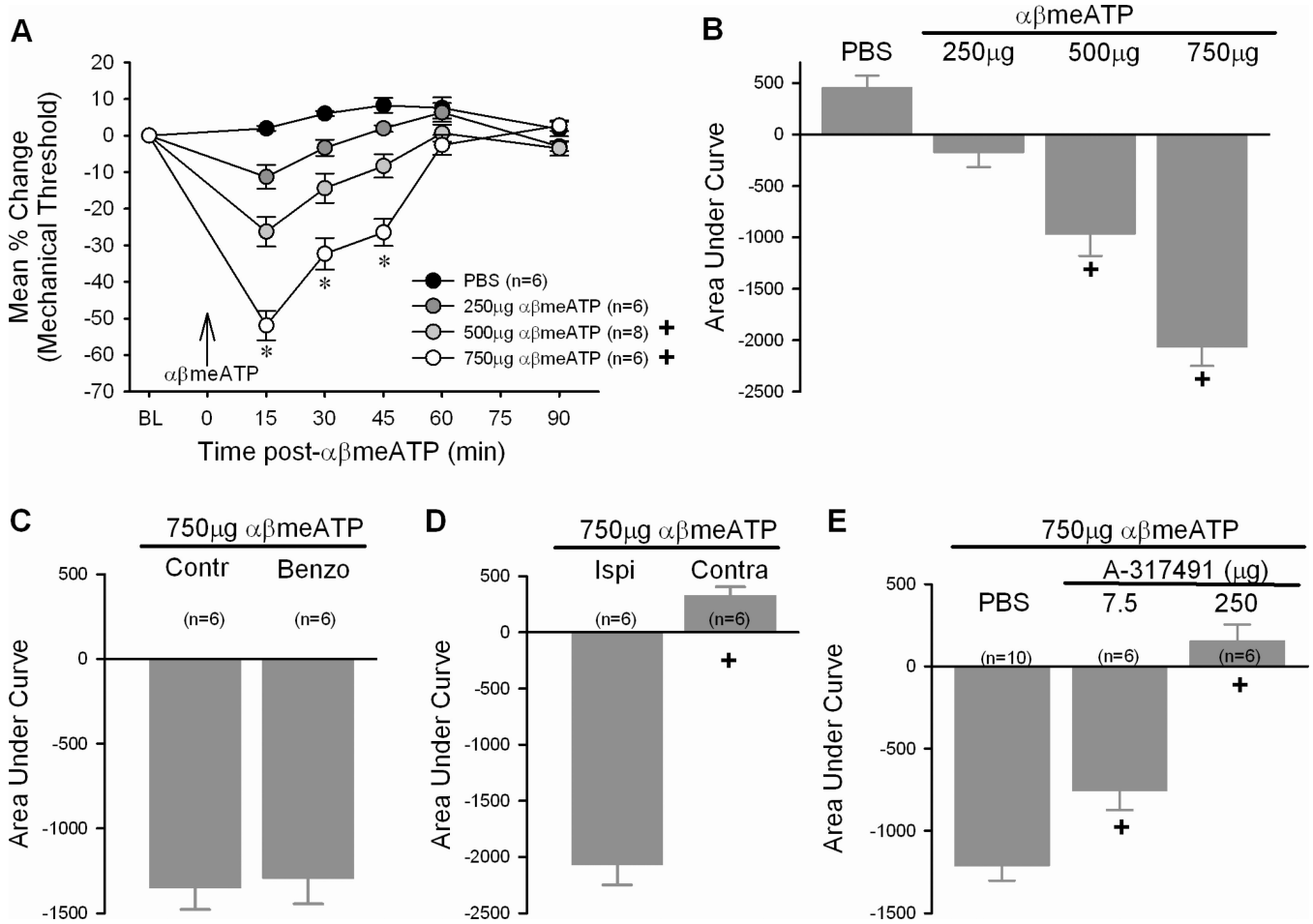

Figure 1.

αβmeATP induces mechanical hyperalgesia in the masseter muscle. (A) The line graphs depict $P2X_3$ agonist αβmeATP-induced changes in mechanical thresholds in the rat masseter muscle. (B) The bar graphs show the overall effects of different doses of αβmeATP on mechanical sensitivity, as shown by Area Under the Curve. (C) The overall effect of intramuscular αβmeATP on masseter sensitivity was examined with topical application of Benzocaine (20%). (D) The overall effect of αβmeATP (750 μg) was compared between the injected and the contralateral muscles. (E) The specificity of αβmeATP was examined with A-317491, a selective $P2X_3$-receptor antagonist. A-317491 was injected into the masseter 5 min prior to αβmeATP. BL indicates baseline 15 min prior to αβmeATP injection. Black arrow indicates αβmeATP injection at 0 min. +, * indicates significant ($P < 0.05$) group and time effects, respectively.

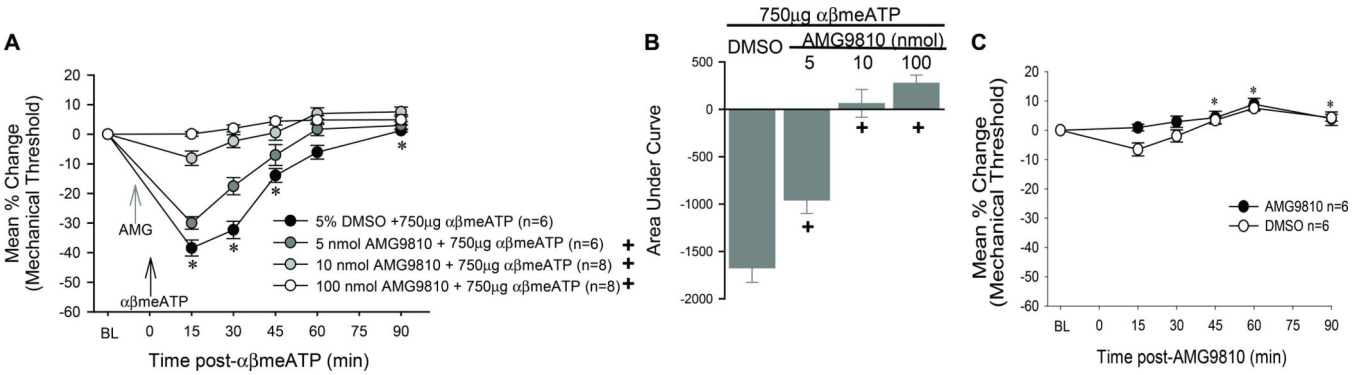

Figure 2.

αβmeATP-induced masseter hyperalgesia involves TRPV1. (A) Line graph shows changes in masseter mechanical thresholds induced by αβmeATP in the presence of the TRPV1 antagonist, AMG9810. (B) Bar graph shows the overall magnitude of drug effect as measured by Area Under Curve (AUC). BL: baseline 15 min prior to αβmeATP injection. Gray arrow: vehicle or antagonist injection 5 min prior to αβmeATP injection. Black arrow: αβmeATP injection at 0 min. (C) Mechanical thresholds were measured at the indicated time points following the injection of AMG9810 (100 nmol) or vehicle. (n = 6/group). +, * indicates significant ($P < 0.05$) group and time effects, respectively.

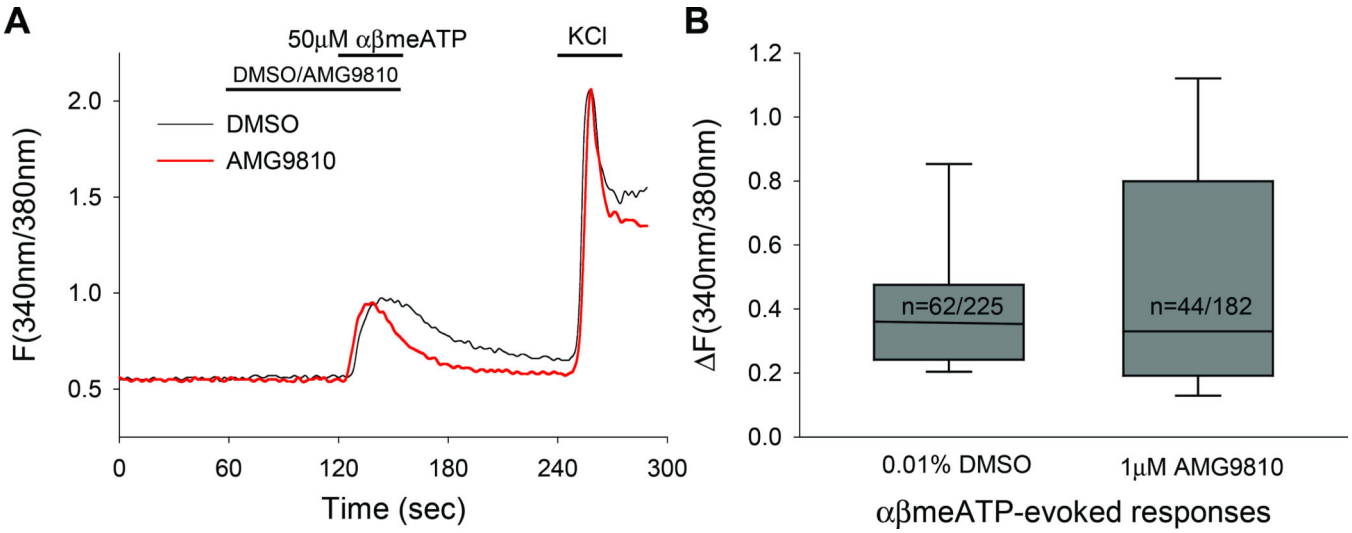

Figure 3.

The effect of AMG9810 on αβmeATP-evoked Ca^{2+} responses. (A) Example traces showing αβmeATP-evoked responses in the presence of vehicle or AMG9810. (B) Box-and-whisker plot demonstrating the magnitude of αβmeATP-evoked responses in the presence or absence of AMG9810 (1 μM). The number of neurons that responded to αβmeATP as a proportion of KCl responders is displayed within the boxes. There were no statistical differences in either the amplitudes or proportion of αβmeATP-evoked responses.

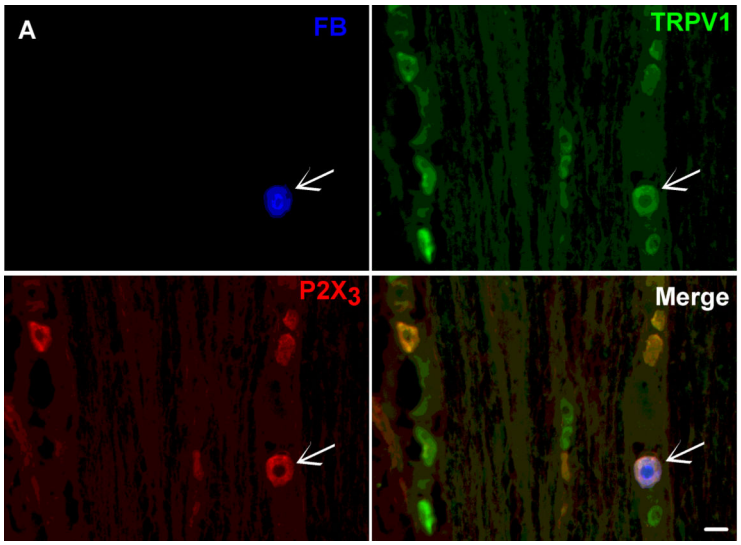

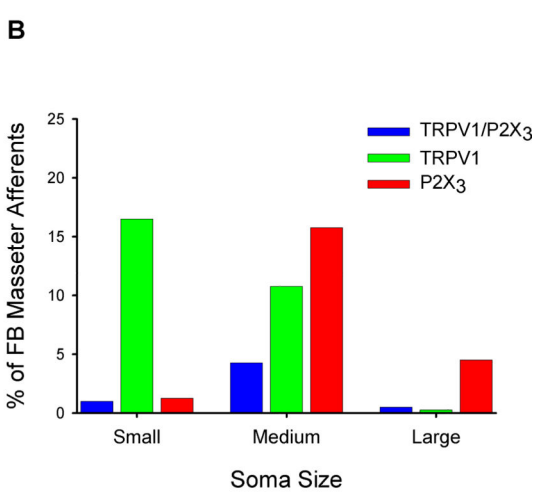

Figure 4.

The somata of masseter afferents labeled by retrograde transport of Fast Blue (FB) were assessed for TRPV1 and $P2X_3$ immunoreactivity. (A) Micrographs illustrating TRPV1 and $P2X_3$ expression in TG neurons, an arrow indicates the FB positive neuron. (B) Soma size distribution of TRPV1 and $P2X_3$ positive masseter afferents in TG based on cell body area (μm^2), small ($<400\mu m^2$), medium (400–1000 μm^2), and large (>1000 μm^2). The expression profile of TRPV1 and $P2X_3$ was assessed in 400 masseter afferents. Scale bar=20μm

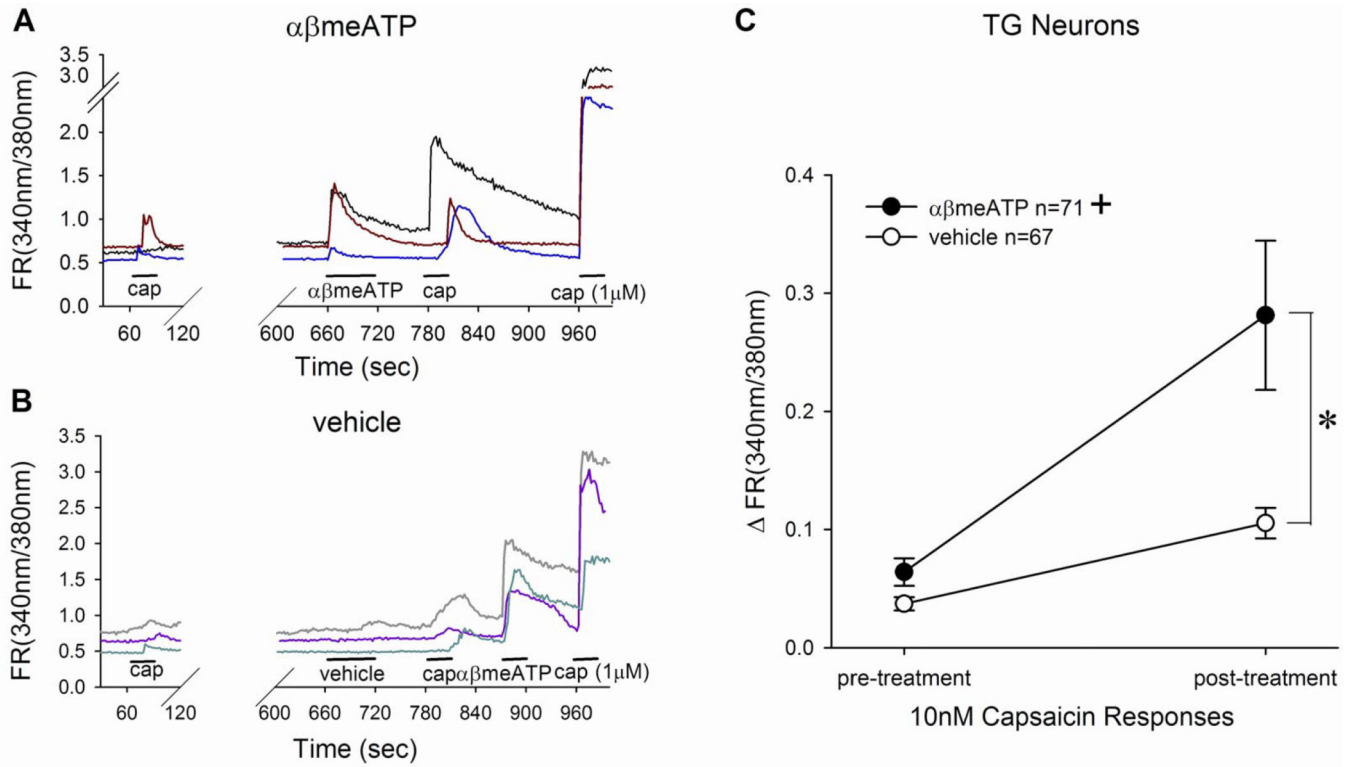

Figure 5.

The effects of αβmeATP on capsaicin-induced Ca^{2+} responses in TG neurons. Representative traces show Fura ratio (FR) from TG neurons in (A) αβmeATP and (B) vehicle treated groups. Each color trace represents responses from one neuron. (C) Averaged changes in Fura response (ΔFR) of the first and second 10 nM capsaicin application in αβmeATP and vehicle-treated groups. This protocol was tested on 12 cultures generated from 12 rats. + denotes significant effect at $P < 0.05$ and * indicates $P < 0.05$ following post-hoc analysis.

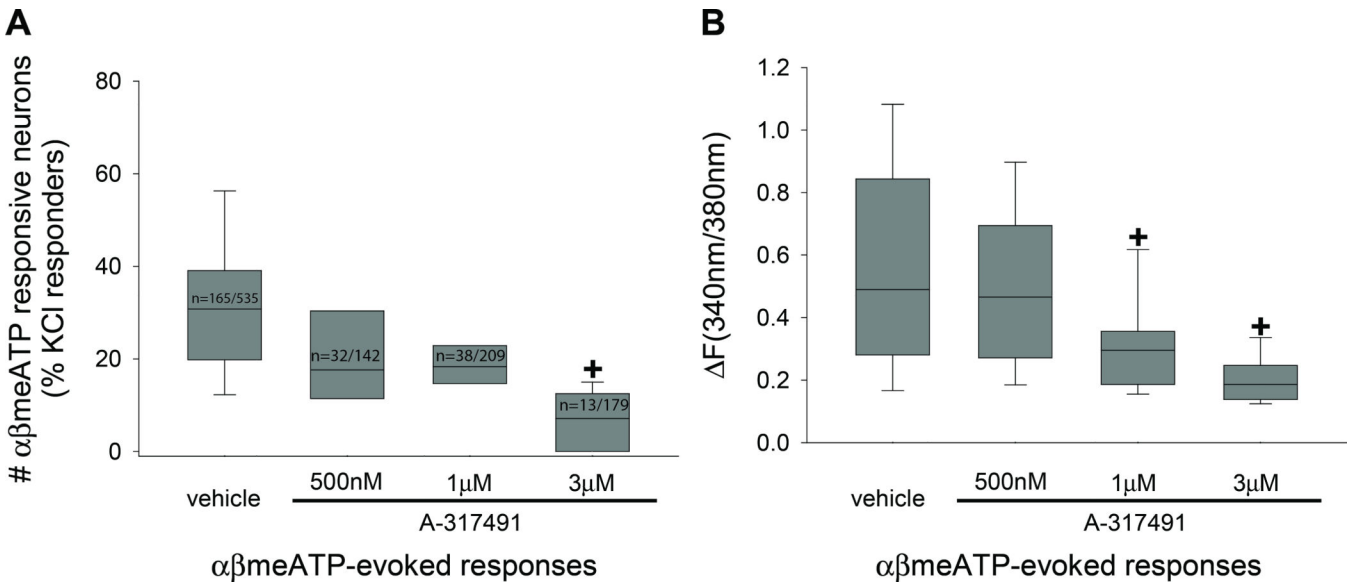

Figure 6.

The αβmeATP effect is mediated by $P2X_3$. (A) The number of responses and (B) the magnitude of responses evoked by 50 μM αβmeATP in the presence of the selective $P2X_3$ antagonist, A-317491. This protocol was tested on 5 cultures generated from 5 rats. The data were analyzed with Kruskal-Wallis One-Way Anova. + indicates significant effect at $P < 0.05$.

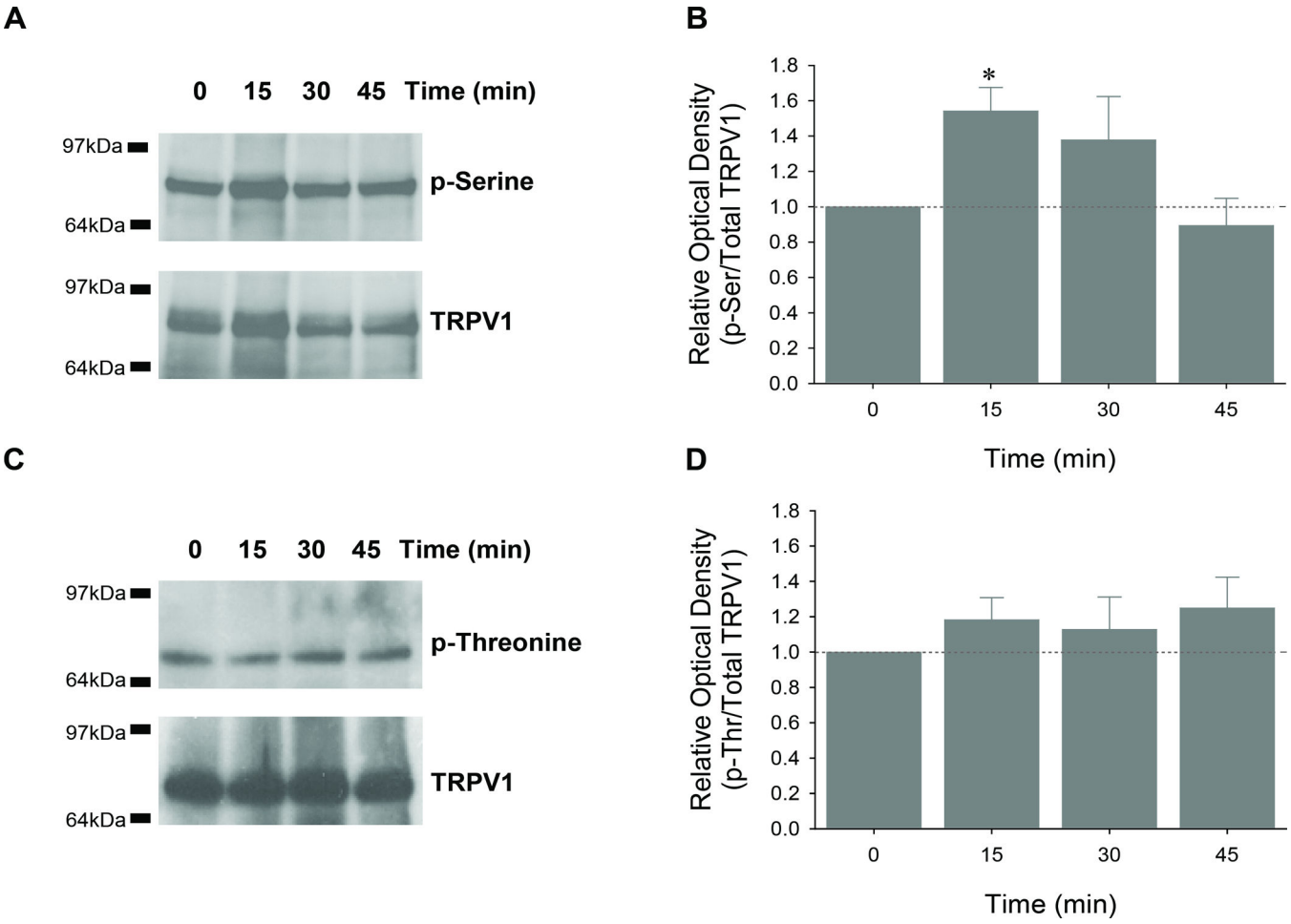

Figure 7.

The effect of αβmeATP on TRPV1 phosphorylation in TG cultures. (A,C) Immunoblots for p-Ser and p-Thr following IP using an anti-TRPV1 antibody (upper). Immunoblots using anti-TRPV1 antibody from the same sample in the upper panel (lower). The samples were collected at the indicated time points following αβmeATP (50 μM) treatment. (B,D) Averaged relative optical densities (p-Ser/TRPV1 and p-Thr/TRPV1) are also shown. * denotes significant effect at $P < 0.05$. n = 6 for each time point.

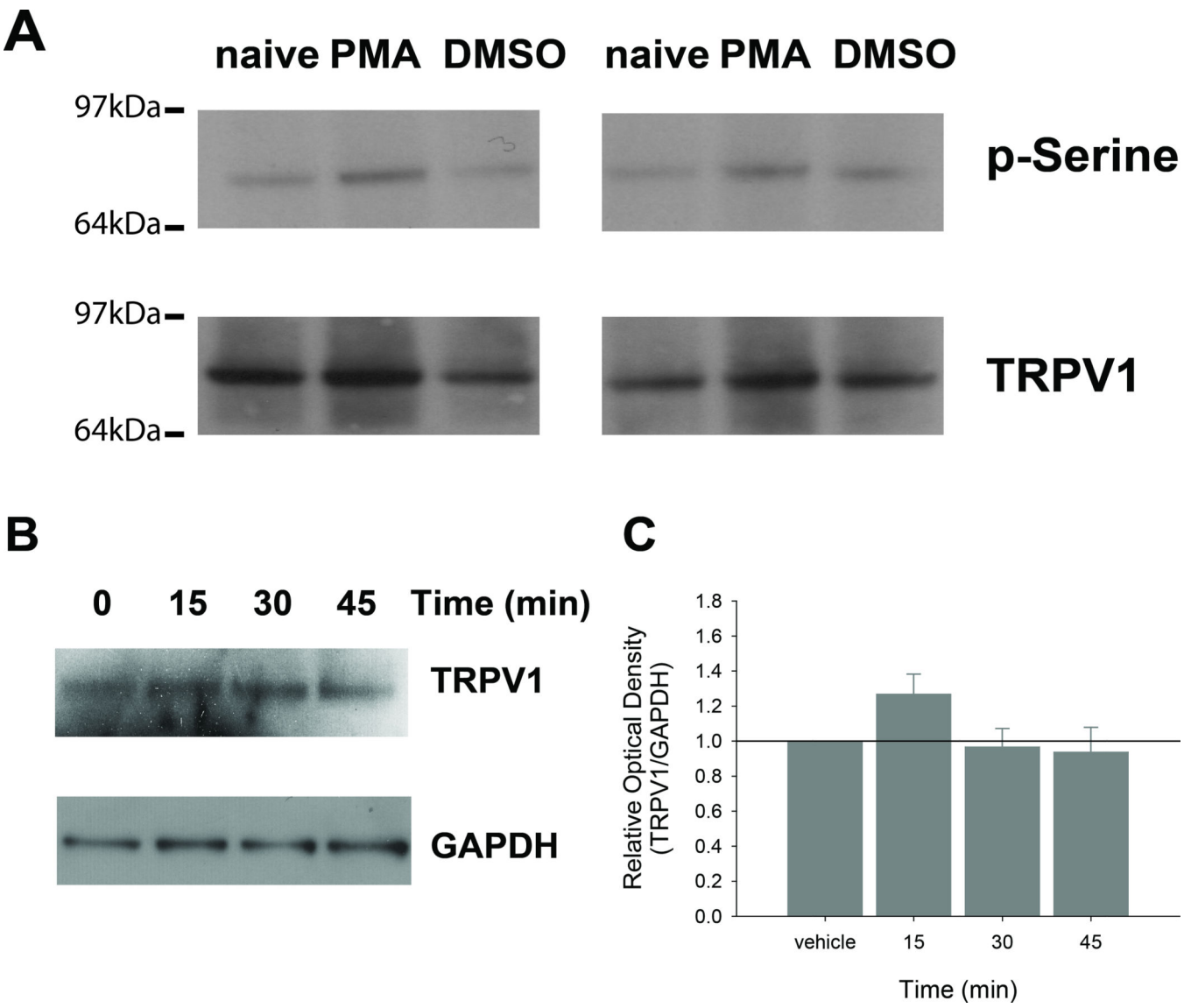

Figure 8.

The effect of PMA on serine phosphorylation, and the effect of αβmeATP on TRPV1 expression in TG cultures. (A) (upper) Immunoblots for p-Ser following IP using an anti-TRPV1 antibody. Samples were either naïve, treated with 1μM PMA or vehicle for 15 min. (lower) Immunoblots of the same sample using an anti-TRPV1 antibody. (B) Representative western blot for TRPV1 (upper) and GAPDH (lower) from the same sample. The samples were collected at the indicated time points following αβmeATP (50 μM) treatment. (C) Averaged relative optical density (TRPV1/GAPDH). n = 3 for each time point.

Table 1

Response Profile of Neurons in Ca^{2+} Imaging Study

	Vehicle/Control	Experimental
% of capsaicin responders that respond to αβmeATP	31% (180/588)	31% (317/703)
% of αβmeATP responders that respond to capsaicin	90% (180/199)	92% (217/235)
Proportion of αβmeATP/capsaicin responders exhibit sensitization	33% (67/180)	37% (71/217)
Proportion of αβmeATP/capsaicin responders exhibit desensitization	62% (111/180)	64% (139/217)